Advanced Materials Research *Online: 2010-12-30*
ISSN: 1662-8985, Vol. 177, pp 32-36
doi:10.4028/www.scientific.net/AMR.177.32

$ZnFe_2O_4$ Modified by $Fe(NO_3)_3$ for the Synthesis of Ionic Ferrofluids

Anrong Wang [1,2], Jian Li [1,b], Qingmei Zhang[1] and Hua Miao[1]

[1] School of Physics Science and Technology, Southwest University, Chongqing 400715, China

[2] School of Physics and Electronic Engineering, Chongqing Threegorges University, Chongqing 404000, China

[b]aizhong@swu.edu.cn

Keywords: Nanoparticle; Coprecipitation; Magnetization; Disphase

Abstract. Weak magnetic $ZnFe_2O_4$ nanoparticles were prepared by coprecipitation and treated with different concentrations of $Fe(NO_3)_3$ solution. Untreated and treated particles were studied using a vibrating sample magnetometer, transmission electron microscope, by X-ray diffraction, X-ray energy dispersive spectroscopy and X photoelectron spectroscopy. The results showed that, after treatment, the $ZnFe_2O_4/\gamma$-Fe_2O_3 forms disphase nanoparticles, with enlarged size, enhanced magnetic properties and with a surface parceled with $Fe(NO_3)_3$. The size of the particles and their magnetic properties are related to the concentration of the treatment solution. The particle size and magnetic properties could be controlled by controlling the concentration of treating solution, therefore nanoparticles can be more widely used.

Introduction

Nanocrystalline materials are those whose grains, grain boundaries and other microscopic structures are on the nanometre scale. Compared with ordinary materials with large particles, nanomaterials have broader applications due to their excellent characteristics such as the small size effect, surface and interface effects, quantum size effect and macroscopic quantum tunneling effect. Nano-$ZnFe_2O_4$ is a traditional ferrite material, which is widely used in electro-magnetic and luminescent materials. Discovered in recent years, nano-zinc ferrite has good catalytic performance [1], acts as a gas sensor [2], can be used for high density magnetic recording media [3] and has applications in biomedicine [4], and for microwave absorbing materials [5]. Therefore, there have been many studies of $ZnFe_2O_4$. However, $ZnFe_2O_4$ is only weakly magnetic. With the rapid development of nano-materials and nano-technology, additional kinds of nano-particle materials have been discovered, contributing to the multi-functionality of nano-composite materials [6]. In recent years, the study of composite oxide nanomaterials has been carried out, using materials such as $Co_{(1-x)}ZnxFe_2O_4$ and $Mn_{(1-x)}ZnxFe_2O_4$ [7], Co/γ-Fe_2O_3 [8], γ-Fe_2O_3/Y_2O_3 [9], γ-Fe_2O_3/SiO_2 [10], PPy/γ-Fe_2O_3 [11]. Xiangxi Bo and others, using $Fe(NO_3)_3 \cdot 9H_2O$ and $Zn(Ac)_2 \cdot 2H_2O$ as raw materials, have described the solvothermal preparation of $ZnFe_2O_4/\gamma$-Fe_2O_3 composite nanoparticles[12]. This article describes the chemical co-precipitation of $ZnFe_2O_4$ nanoparticles as a precursor, and using $Fe(NO_3)_3$ solution to modify the $ZnFe_2O_4$ nanoparticles. The modified magnetic nanoparticles are a combination of γ-Fe_2O_3 and $ZnFe_2O$, with strongly magnetic γ-Fe_2O_3 inside and $ZnFe_2O_4$outside.

Experimental

Preparation of precursor nanometer particles. $ZnFe_2O_4$ nanoparticles are prepared by co-precipitation from ferric chloride $FeCl_3 \cdot 6H_2O$, zinc chloride $ZnCl_2$ and sodium hydroxide NaOH with a mole ratio of 2:1 between Fe^{3+} and Zn^{2+}. The chemical reaction follows the equation:

$$2FeCl_3 + ZnCl_2 + 8NaOH \underset{\Delta}{=} ZnFe_2O_4 + 8NaCl + 4H_2O \quad (1)$$

Two hours after cooling, the sediment was repeatedly washed to remove Na^+, NO_3^- and Cl^-. $0^{\#}$ nanoparticles samples were obtained by dehydration through natural drying.

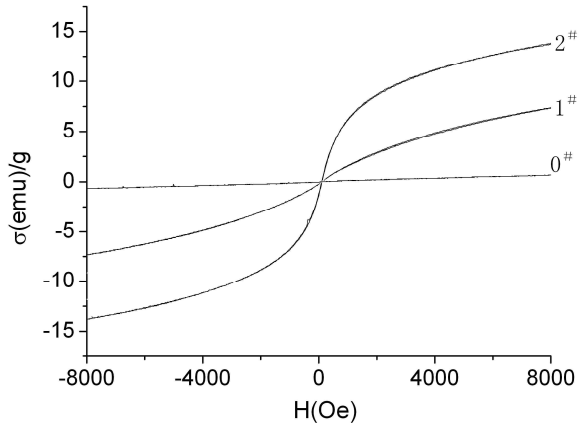

Figure 1. The magnetic properties of the particle samples

Preparation of $ZnFe_2O_4/\gamma$-Fe_2O_3 disphase particles. The sediment prepared above was divided into two halves. These were boiled for 30 minutes with 0.25M then 0.5M $Fe(NO_3)_3$ solutions. $1^{\#}$ and $2^{\#}$ nanoparticle samples were obtained by cooling, centrifuging, adding acetone to assist dehydration, natural drying and grinding into powder.

Characterization. A composition analysis was performed at room temperature on particles $0^{\#}$, $1^{\#}$ and $2^{\#}$ with a Norton 8000 energy dispersive X-ray detector (EDX). The surface composition analysis was carried out using an ESCALAB 250 X-ray photoelectron spectroscope (XPS), crystallographic analysis with a D/MAX-3C X-ray diffraction (XDR), analysis of particle size with a H-600 transmission electron microscope (TEM), and the magnetization curve of the strong magnetic particles was measured using a HH-15 VSM.

Results and Analysis

Magnetization curve measurement. Figure 1 shows the ratio magnetization curve of the samples of particles. Sample $0^{\#}$ particles, untreated with $Fe(NO_3)_3$, are weakly paramagnetic, with magnetization that can be written as:

$$M = \chi H \tag{2}$$

The $1^{\#}$ and $2^{\#}$ particles are super-paramagnetic after treatment with $Fe(NO_3)_3$. $1^{\#}$ and $2^{\#}$ particle samples have clearly enhance magnetism over $0^{\#}$ and the magnetism of sample $2^{\#}$ is greater than $1^{\#}$, which indicates that Zn transfer takes place in the $Fe(NO_3)_3$ process. The particles generate γ-Fe_2O_3 [13] and the magnetization increases after the treatment since this depends on the concentration of $Fe(NO_3)_3$. The higher the concentration, the higher is the content of γ-Fe_2O_3, so the magnetization of particles is stronger.

TEM. The TEM of the sample particles is shown in Figure 2, with the TEM photographs of $0^{\#}$, $1^{\#}$ and $2^{\#}$ given in figure 2 (a), Figure 2 (b) and figure 2 (c), respectively.

TEM observations show that the particles are spherical. The particles sizes form a logarithmic normal distribution.

$$\frac{d\varphi}{d\ln x} = \frac{1}{\sqrt{2\pi}\ln\sigma_g}\exp[-\frac{(\ln x - \ln x_g)^2}{2\ln^2\sigma_g}] \tag{3}$$

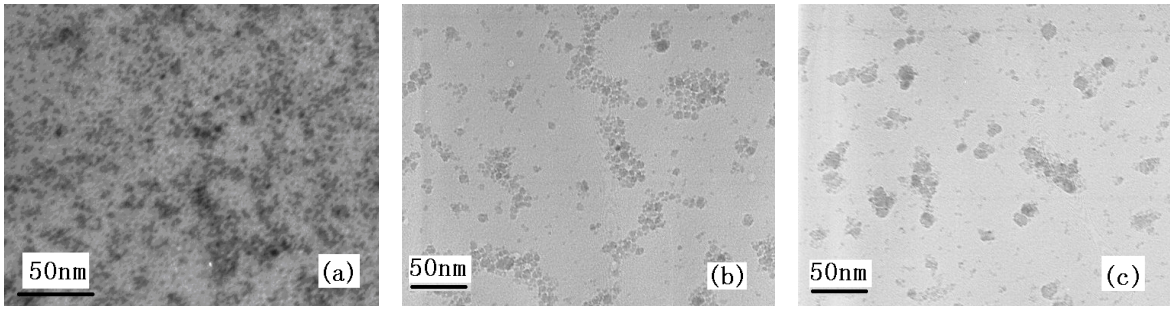

Figure 2. Typical TEM micrographs of the particles (a) sample $0^{\#}$ particles; (b) sample $1^{\#}$ particles; and (c) sample $2^{\#}$ particles

where x is the nanoparticle diameter, x_g is the geometric mean diameter, d is the ratio of lnx to the $lnx+dlnx$ for the whole particle. σ_g is the particle size geometric standard deviation. The $0^{\#}$, $1^{\#}$ and $2^{\#}$ particle sample sizes are shown in Table 1.

Table 1 Particle sizes of samples

Samples	$0^{\#}$	$1^{\#}$	$2^{\#}$
Particles size (nm)	4.22	4.70	6.17

Table 2 EDX Data (atom%)

Element	$0^{\#}$	$1^{\#}$	$2^{\#}$
Fe	63.10	85.42	81.70
Zn	36.90	14.58	18.30

Table 3 XPS data (atom%)

Element	$0^{\#}$	$1^{\#}$	$2^{\#}$
Fe	61.10	90.78	83.04
Zn	38.90	9.22	16.95

The average size of the untreated $0^{\#}$ particle is 4.22nm, but the average size of the treated particle increases with increasing concentration of the $Fe(NO_3)_3$ solution, which indicates that particle treatment boosts reunion growth, and thereby increases the particle size.

XRD. X-ray diffraction (XRD) spectra of the samples are shown in Figure 3.

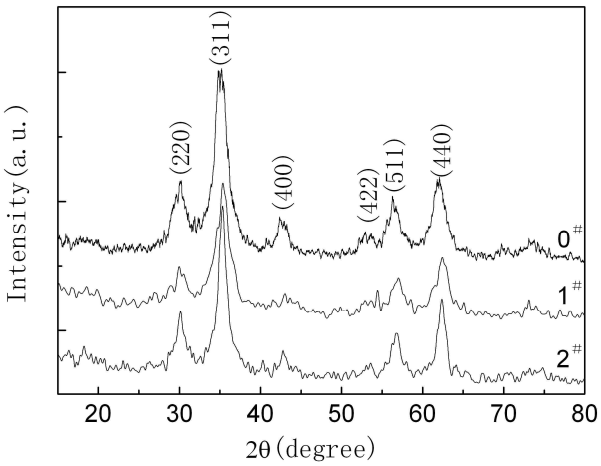

Figure 3. XRD spectra of the particles

In Figure 3, we can see that sample $0^{\#}$ particles are $ZnFe_2O_4$, since the peaks for the treated particles and $ZnFe_2O_4$ are basically the same. The decline of the XRD diffraction peak in samples $1^{\#}$ and $2^{\#}$ shows an increase of the non-crystalline $Fe(NO_3)_3$ component in the treated particles. However, the diffraction peak in sample $2^{\#}$ is stronger than that in sample $1^{\#}$, which shows the spectral peak of γ-Fe_2O_3 in the treated particles. The γ-Fe_2O_3 content of sample $2^{\#}$ is larger, so the diffraction peak is stronger. The peaks of $ZnFe_2O_4$ and γ-Fe_2O_3 are very close, so they are difficult to distinguish in the XRD spectra.

EDX. The samples were analyzed by EDX and the ratio between the Zn and Fe atoms is shown in Table 2.

From Table 2 we can see that the particles are mainly composed of Zn and Fe and the atomic ratio of Zn and Fe is about 1:2 in the sample $0^{\#}$. The sample $0^{\#}$ particles consist of $ZnFe_2O_4$ and the analytical results are consistent with the XRD. However, the content of Fe atoms increases and the content of Zn atoms decreases significantly in the treated particles, partly because the internal Zn transfer may produce γ-Fe_2O_3 in the treated particles and partly because $Fe(NO_3)_3$ may be adsorbed on to the surface[15]so that the composition of particles changes. The adsorptive non-magnetic $Fe(NO_3)_3$ decreases on the surface of sample $2^{\#}$, so the content of Zn is higher than in sample $1^{\#}$, and the magnetic properties increase as a result.

XPS. The XPS spectra of the particles are shown in Figure 4 and the data obtained from the XPS spectral analysis are in Tables 3 and 4.

From Table 3 we can see that the atomic ratio of Zn and Fe is about 1:2 in sample $0^{\#}$, the same as

the EDX result, indicating that the surface composition of sample $0^{\#}$ particles and the overall composition are both $ZnFe_2O_4$. The Fe atom content of the surface of the treated particles of samples $1^{\#}$ and $2^{\#}$ also increased significantly along with a decrease of Zn atoms. The concentration of Fe atoms in the surface layer of the particles is greater than that of the complete particle, which shows that the surface of the treated particles has also adsorbed $Fe(NO_3)_3$.

Figure 4 (a) shows the Zn2p peaks, from which we can see that the peaks are significantly weaker in the treated particles. The position of the Zn2p peaks of the precursor $ZnFe_2O_4$ particles is the same as that of the treated particles. Therefore, the Zn of the treated particles is still the Zn of $ZnFe_2O_4$, which shows that the surface of the treated particles is still $ZnFe_2O_4$. However, the $ZnFe_2O_4$ content of the surface of the treated particles decreased significantly.

Figure 4 (b) shows the N1s peaks of the treated particles, with the surface chemical composition of $ZnFe_2O_4$ particles different from the treated particles, with Zn, Fe, O on the surface of $ZnFe_2O_4$ particles and little additional N. The N1s binding energy of the treated particles is the same as the N1s binding energy of $Fe(NO_3)_3$, which further indicates that there is a small amount of $Fe(NO_3)_3$ absorbed after the $Fe(NO_3)_3$ treatment.

Table 4 Binding energy data from XPS (eV)

	$Zn2p_3$		$Fe2p_3$	O1s		N1s
$0^{\#}$	1020.86	710.95		530.48		
$1^{\#}$	1020.53	711.22	529.81	530.61	532.59	406.76
$2^{\#}$	1020.63	711.78	529.74	530.29	532.22	406.53
γ-Fe_2O_3[15]		711.3	530.0			
$Fe(NO_3)_3$[14]		710.09			532.93	406.65

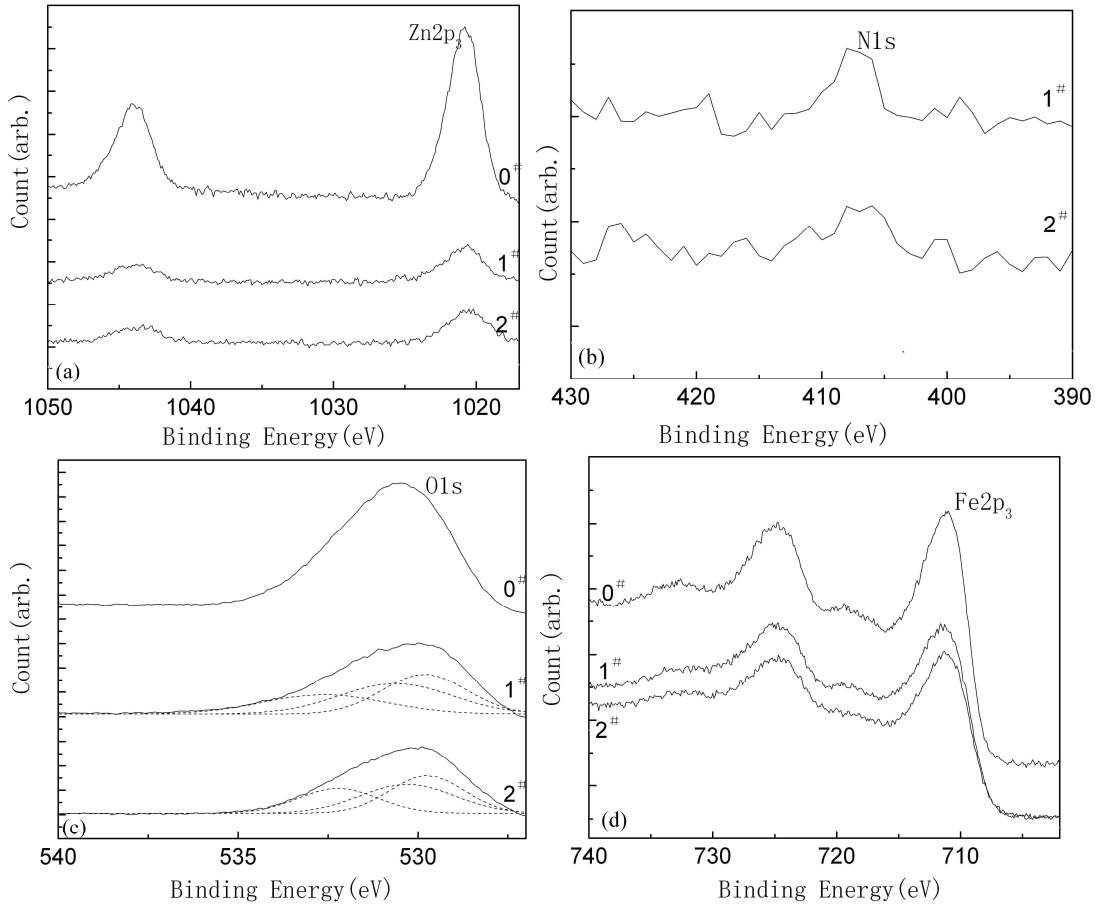

Figure 4 . XPS spectra of the particles. (a) Zn2p lines; (b) N1s lines of treated particles; (c) O1s lines; and (d) Fe2p lines.

From Figure 4 (c), we can see that the position of the O1s peaks of the precursor $ZnFe_2O_4$ particles are different to those of the treated particles. Therefore, the oxygen atoms of the treated particles consist not only of O from $ZnFe_2O_4$, but also from new phases. Gaussian decomposition of the XPS data, together with information from the preparation and EDX results, shows that the surface of the treated particles contains $Fe(NO_3)_3$ and γ-Fe_2O_3 with O1s binding energies 532.93eV and 530.0eV, respectively.

Figure 4 (d) shows the Fe2p peaks. Because the Fe2p peaks do not display a Gaussian distribution, it is difficult to make a Gaussian decomposition. From the figure we can see that the $Fe2p_3$ binding energy of the treated particles and the $Fe2p_3$ binding energy of γ-Fe_2O_3 are the same. This shows that the $Fe2p_3$ binding energy of the surface layer of $ZnFe_2O_4$ is close to that of γ-Fe_2O_3 (ΔE=711.3-710.95 = 0.35eV), while $Fe(NO_3)_3$ contains such a small amount that the $Fe2p_3$ peaks of $ZnFe_2O_4$ and $Fe(NO_3)_3$ do not show up in the spectra.

The XPS analytical results show that the treated nano-particles are mainly composed of γ-Fe_2O_3 and $ZnFe_2O_4$, with a small amount of $Fe(NO_3)_3$ in addition.

Conclusion

From this experimental analysis and discussion we can draw the following conclusions:

In the process of $Fe(NO_3)_3$ treatment, Zn is transferred, γ-Fe_2O_3 is produced and the magnetization of the particles are enhanced. The magnetization depends on the concentration of the solution of $Fe(NO_3)_3$; the higher the concentration, the greater the content of γ-Fe_2O_3 and the stronger the magnetization.

The growth of the treated particles and hence the increase of the particle size, also depends on the concentration of the $Fe(NO_3)_3$ solution; the higher the concentration, the greater the size of the particles. The treated particles consist of $ZnFe_2O_4$/γ-Fe_2O_3 disphase nanoparticles, with some additional $Fe(NO_3)_3$ adsorbed on the surface.

$Fe(NO_3)_3$ treatment not only improves the particle surface acid resistance of $ZnFe_2O_4$-γ-Fe_2O_3 composite nano-particles, but also, by changing the concentration of the $Fe(NO_3)_3$ solution, change the particle size and magnetic properties of the $ZnFe_2O_4$/γ-Fe_2O_3 nano-particles, which is of vital significance for expansion of nano-particles into other areas of application.

References

[1] S.W. Caoa, Y.J. Zhua and G.F. Cheng, et al: Journal of Hazardous Materials. Vol. 171(2009), p. 431.
[2] S. Zhuiykov, T. Ono, N. Yamazoe, et al: Solid State Ionics Vol. 152– 153(2002), p. 801.
[3] A. Moser, K. Takano, D.T.Margulies, et al: J. Phys. D: Appl. Phys. Vol. 35(2002), p. R157.
[4] J.M. Bai, J.P. Wang: Appl. Phys. Lett. Vol. 87(2005), p. 152502.
[5] R.C. Che, L.M. Peng, X.F. Duan, et al: Adv. Mater. Vol. 16(2004), p. 401.
[6] W.D. Ke, H. Hao, Y. Kuai, et al: China Powder Industry. Vol. 5(2008), p. 19-23(in Chinese).
[7] R. Arulmurugan, B. Jeyadevan, G. Vaidyanathan, et al: J. Mag. Mag. Mater. Vol. 288(2005), p. 470.
[8] Z.H. Jing , S.H. Wu: Materials Letters. Vol. 60(2006), p. 952.
[9] S.W. Tao, X.Q. Liu, X.F. Chu, et al: Sensors and Actuators B Vol. 61(1999), p. 33.
[10] X.J. Xu, J. Wang, C.Q. Yang, et al: Journal Alloys and Compounds. Vol. 468(2009), p. 414.
[11] H. Yuvaraj, M.H. Woo, E.J. Park, Y.T. Jeong, et al: Europ. Polym. J. Vol. 44(2008), p. 637.
[12] X.X. Bo, G.S. Li, X.Q. Qiu, et al: Journal of Solid State Chemistry. Vol. 180 (2007), p.1038.
[13] M.H. Sousa, F.A. Tourinho and J.C. Rubim: Journal of Raman Spectroscopy. Vol. 31(2000), p.185.
[14] A.R. Wang, J. Li, Y. Wang: Journal of Instrumental Analysi. Vol. 25(2006), p. 35(in Chinese).
[15] C.D. Wagner, W.M. Riggs, L.E. Davis, et al: HandBook of X-Ray Photoelectron Spectroscopy (Perkin-Elmer Corporation Physical Electronics Division6509 Flying Cloud Drive Eden, Prairie, Minnesota 55344, USA, 1979).